The bone marrow niche regulates redox and energy balance in MLL::AF9 leukemia stem cells

Authors:
Ana C. Viñado[1,2,*], Isabel A. Calvo[1,2,*], Itziar Cenzano[1], Danel Olaverri[3], Miguel Cocera[1], Patxi San Martin-Uriz[1], Juan P. Romero[1], Amaia Vilas-Zornoza[1], Laura Vera[4], Nuria Gomez-Cebrian[5], Leonor Puchades-Carrasco[5], Livia E. Lisi Vega[6], Iñigo Apaolaza[3,7], Pablo Valera[1], Elisabeth Guruceaga[1], Froilan Granero-Molto[4,8,9], Purificacion Ripalda-Cemborain[4,9], Tamara J. Luck[10,11], Lars Bullinger[10-11], Francisco J. Planes[3,7], José J. Rifon[12], Simón Méndez-Ferrer[6], Rushdia Z. Yusuf[13,#], Ana Pardo-Saganta[14-16,#], Felipe Prosper[1,2,12,,#], Borja Saez[1,2,#,‡]

‡ Correspondence to: Borja Saez, CIMA Universidad de Navarra, Avda. Pio XII 55, 31008, Pamplona, Navarra, Spain. E-mail: bsaezoch@unav.es. Phone: +34 948194700 (811020).

Affiliations
1. Hematology-Oncology Program, CIMA Universidad de Navarra, Instituto de Investigación Sanitaria de Navarra (IdiSNA), 31008, Pamplona, Spain.
2. Centro de Investigación Biomédica en Red de Cáncer, CIBERONC.
3. Tecnun Universidad de Navarra, School of Engineering, 20018, San Sebastian, Spain.
4. Regenerative Medicine Program, CIMA Universidad de Navarra, Instituto de Investigación Sanitaria de Navarra (IdiSNA), 31008, Pamplona, Spain.
5. Drug Discovery Unit, Instituto de Investigación Sanitaria La Fe. 46026, Valencia, Spain.
6. Wellcome-MRC Cambridge Stem Cell Institute, Department of Hematology, University of Cambridge, and NHS Blood and Transplant, Cambridge CB2 0AW, United Kingdom.
7. Universidad de Navarra, Centro de Ingeniería Biomédica and DATAI Instituto de Ciencia de los Datos e Inteligencia Artificial, 31008, Pamplona, Spain.
8. Cell Therapy Area, Clínica Universidad de Navarra. 31008, Pamplona, Spain.
9. Department of Orthopaedic Surgery and Traumatology, Clínica Universidad de Navarra. 31008, Pamplona, Spain.
10. Charité – Universitätsmedizin Berlin, corporate member of Freie Universität Berlin, Humboldt-Universität zu Berlin, and Berlin Institute of Health, Department of Hematology, Oncology, and Cancer Immunology, Berlin, Germany.
11. German Cancer Consortium (DKTK) and German Cancer Research Center (DKFZ), Heidelberg, Germany.
12. Department of Hematology, Cell Therapy and Center of Cancer of the University of Navarra, Clínica Universidad de Navarra (CCUN). 31008, Pamplona, Spain.
13. Dana Farber Cancer Institute, 450 Brookline Ave, Boston, MA 02215, United States
14. Institute for Lung Health (ILH), Justus Liebig University Giessen, 35392, Germany.
15. Universities of Giessen and Marburg Lung Center (UGMLC), Giessen, 35392, Germany.
16. German Center for Lung Research (DZL), Giessen, 35392, Germany.

* Equal first author contribution.
# Senior author with equal contribution.

Supp. Figure 1

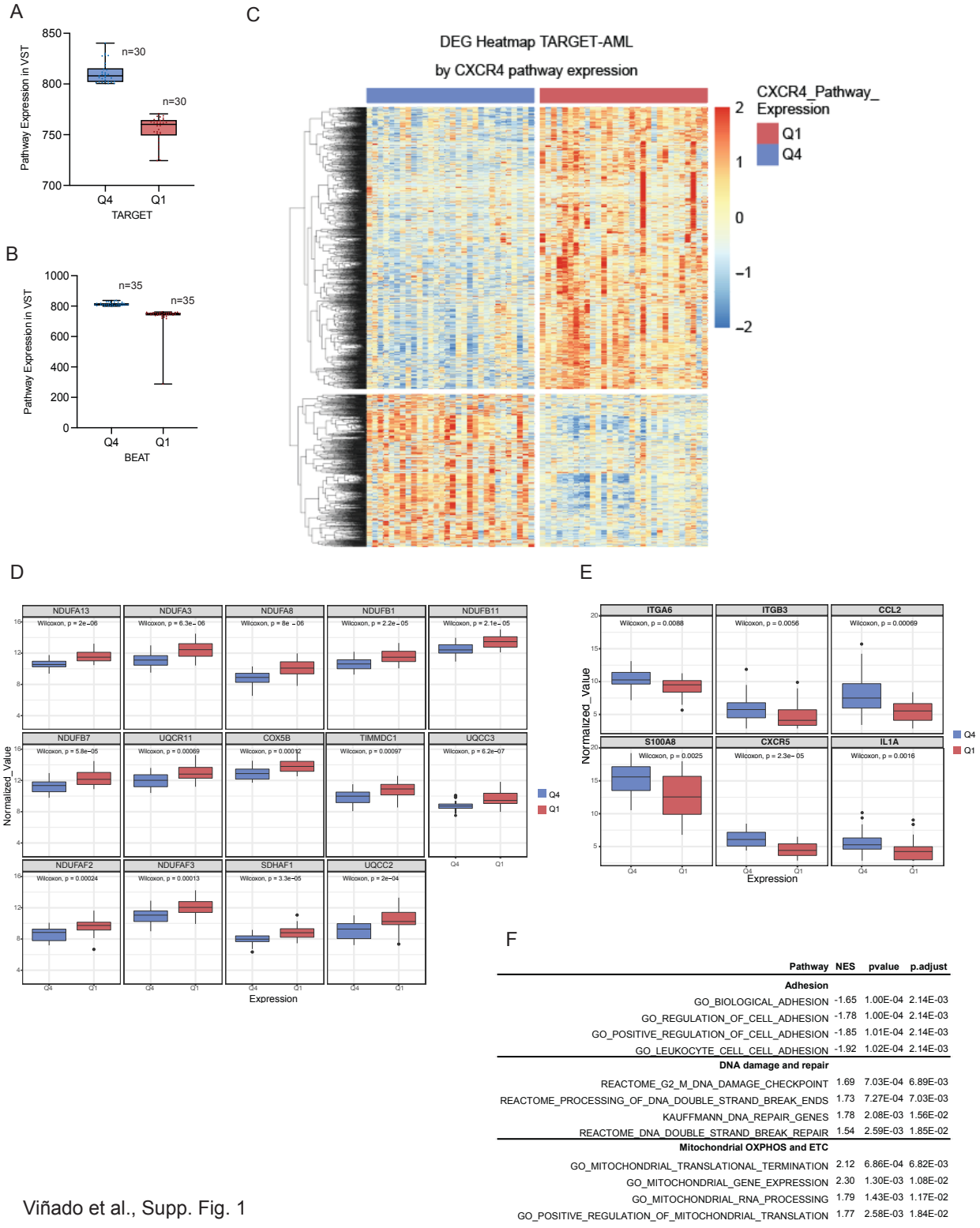

F

Pathway	NES	pvalue	p.adjust
Adhesion			
GO_BIOLOGICAL_ADHESION	-1.65	1.00E-04	2.14E-03
GO_REGULATION_OF_CELL_ADHESION	-1.78	1.00E-04	2.14E-03
GO_POSITIVE_REGULATION_OF_CELL_ADHESION	-1.85	1.01E-04	2.14E-03
GO_LEUKOCYTE_CELL_CELL_ADHESION	-1.92	1.02E-04	2.14E-03
DNA damage and repair			
REACTOME_G2_M_DNA_DAMAGE_CHECKPOINT	1.69	7.03E-04	6.89E-03
REACTOME_PROCESSING_OF_DNA_DOUBLE_STRAND_BREAK_ENDS	1.73	7.27E-04	7.03E-03
KAUFFMANN_DNA_REPAIR_GENES	1.78	2.08E-03	1.56E-02
REACTOME_DNA_DOUBLE_STRAND_BREAK_REPAIR	1.54	2.59E-03	1.85E-02
Mitochondrial OXPHOS and ETC			
GO_MITOCHONDRIAL_TRANSLATIONAL_TERMINATION	2.12	6.86E-04	6.82E-03
GO_MITOCHONDRIAL_GENE_EXPRESSION	2.30	1.30E-03	1.08E-02
GO_MITOCHONDRIAL_RNA_PROCESSING	1.79	1.43E-03	1.17E-02
GO_POSITIVE_REGULATION_OF_MITOCHONDRIAL_TRANSLATION	1.77	2.58E-03	1.84E-02

Viñado et al., Supp. Fig. 1

Supplementary Figure 1. Transcriptional analysis of human pediatric and adult AML with low CXCR4 pathway activation show conserved features with the Prx1-Cxcl12-Mut mice (Related to Fig. 1). (A,B) Samples from the **(A)** TARGET and **(B)** BEAT datasets segregated by the activation of the CXCR4 pathway (Q1 low CXCR4 activation; Q4 high CXCR4 activation). **(C)** Heatmap showing the differentially expressed genes from RNA-seq performed in leukemic cells with low CXCR4 pathway activation from the TARGET dataset. **(D)** Differential expression of genes associated with electron transport chain complexes and related assembly proteins in leukemic cells with low CXCR4 pathway activation from the TARGET dataset. **(E)** Differential expression of genes associated with cell adhesion in leukemic cells with low CXCR4 pathway activation from the TARGET dataset. **(F)** Gene set enrichment analysis (GSEA) of the transcriptional signature of leukemic cells showing a deficiency in signatures related with cell adhesion and migration, as well as, an enrichment of pathways related to cell cycle, DNA damage and repair and mitochondrial respiration in patients with low CXCR4 pathway activation from the BEAT dataset.

Supp. Figure 2

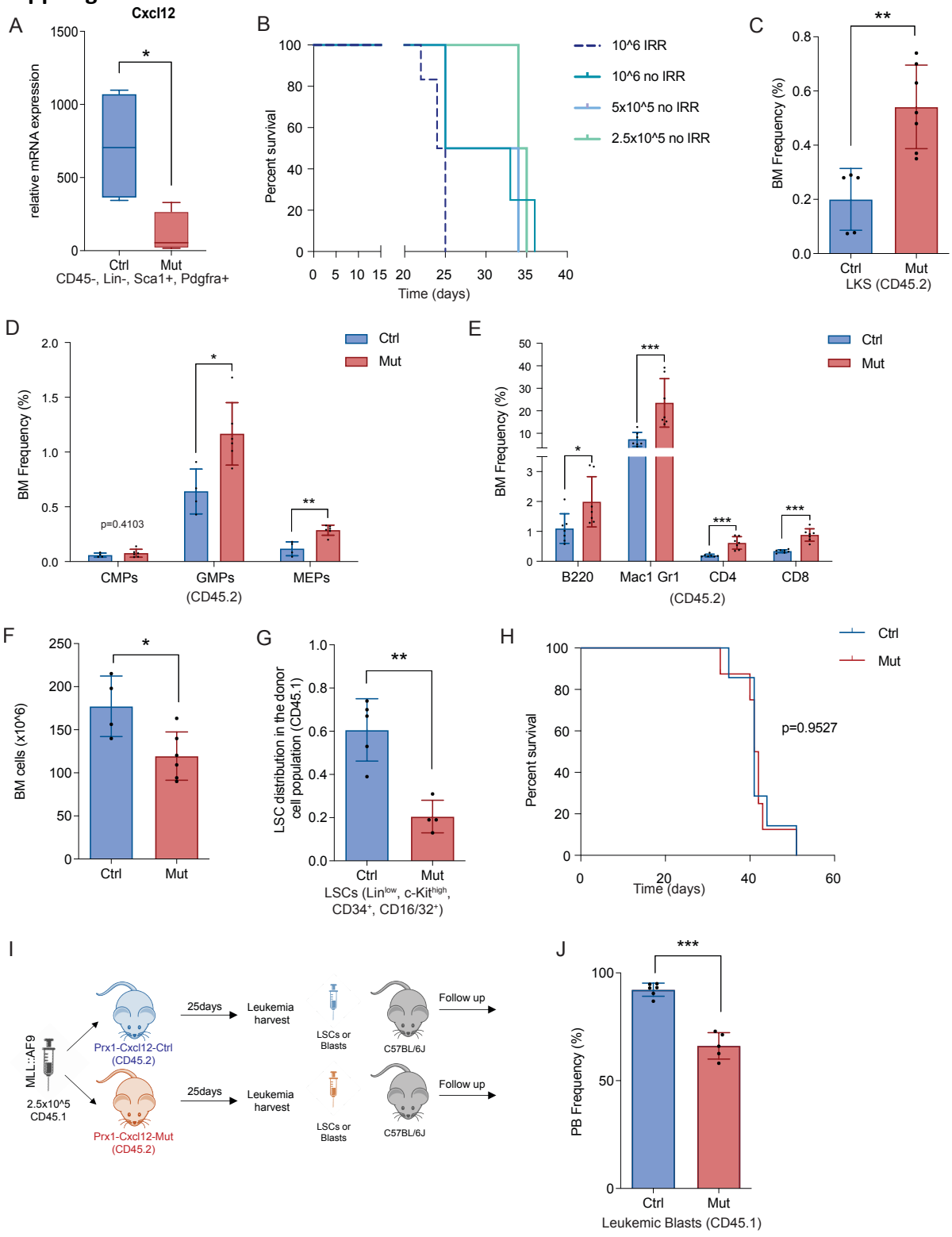

Viñado et al., Supp. Fig. 2

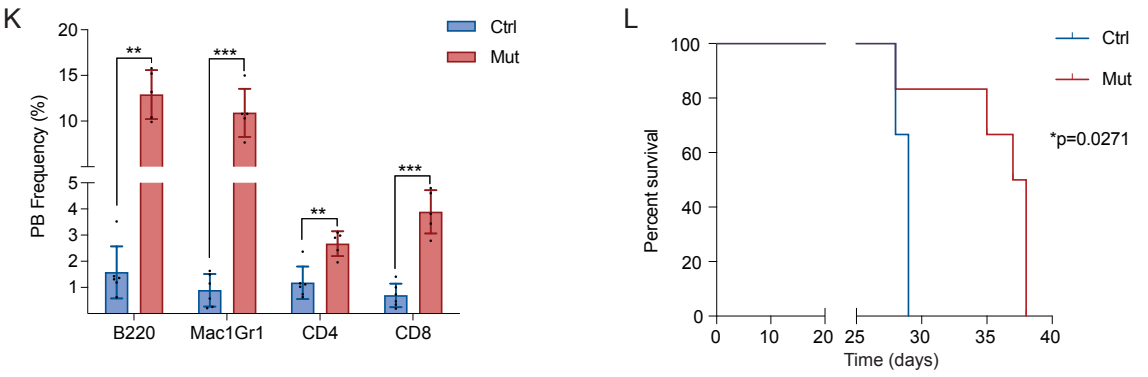

Viñado et al., Supp. Fig. 2 cont.

Supplementary Figure 2. Prx1^{+} mesenchymal cells are integral part of the LSC niche (Related to Fig. 2). (A) mRNA expression of *Cxcl12* in mesenchymal stromal cells (CD45^{-}, Lin^{-}, Sca1^{+}, Pdgfra^{+}) from Prx1-Cxcl12-Mut and Prx1-Cxcl12-Ctrl mice. **(B)** Kaplan-Meier curve showing survival of C57BL/6J mice (n=4-6) transplanted with 10^6, $5x10^5$ or $2.5x10^5$ MLL::AF9 cells with and without irradiation. **(C-E)** Bone marrow (BM) analysis showing the frequency of non-leukemic cells (CD45.2): **(C)** Lin^{-}, cKit^{+}, Sca1^{+} (LKS) cells; **(D)** common myeloid progenitors (CMPs), granulocyte macrophage progenitors (GMPs) and megakaryocyte erythroid progenitors (MEPs) and **(E)** B220, Mac1-Gr1, CD4 and CD8 cells in the Prx1-Cxcl12-Ctrl and Prx1-Cxcl12-Mut mice 25 days after leukemia induction. **(F,G)** Bone marrow analysis showing: **(F)** total cellularity and **(G)** Frequency of LSCs (CD45.1+, Linlow, c-Kithigh, Sca1-, CD34+, CD16/32+) in the CD45.1 leukemic clone. **(H)** Kaplan-Meier curve showing survival of Prx1-Cxcl12-Ctrl (n=7) and Prx1-Cxcl12-Mut (n=8) transplanted with $2x10^5$ MLL::AF9 cells. **(I)** Schematic overview of the experimental design for serial AML induction in C57BL/6J mice with MLL::AF9 cells isolated from the Prx1-Cxcl12-Ctrl and Prx1-Cxcl12-Mut mice. **(J)** Infiltration of leukemic cells in the peripheral blood (PB) 30 days post-transplantation of equal numbers of CD45.1 leukemic cells from Prx1-Cxcl12-Mut and Prx1-

Cxcl12-Ctrl animals. **(K)** Peripheral blood (PB) analysis showing the frequency of non-leukemic B220, Mac1-Gr1, CD4 and CD8 cells in C57BL/6J mice transplanted with CD45.1^{+} leukemic cells from the Prx1-Cxcl12-Ctrl and Prx1-Cxcl12-Mut mice. **(L)** Kaplan-Meier curve showing survival of C57BL6J mice (n=6/group) transplanted with equal numbers of CD45.1^{+} leukemic cells from Prx1-Cxcl12-Ctrl (n=5) and Prx1-Cxcl12-Mut (n=5) animals. Data are representative of at least 2 independent experiments. n=5 to 6 mice per genotype per experiment unless otherwise stated. Data are represented as mean and SD. * P< .05; ** P< .01; *** P< .001.

Supp. Figure 3

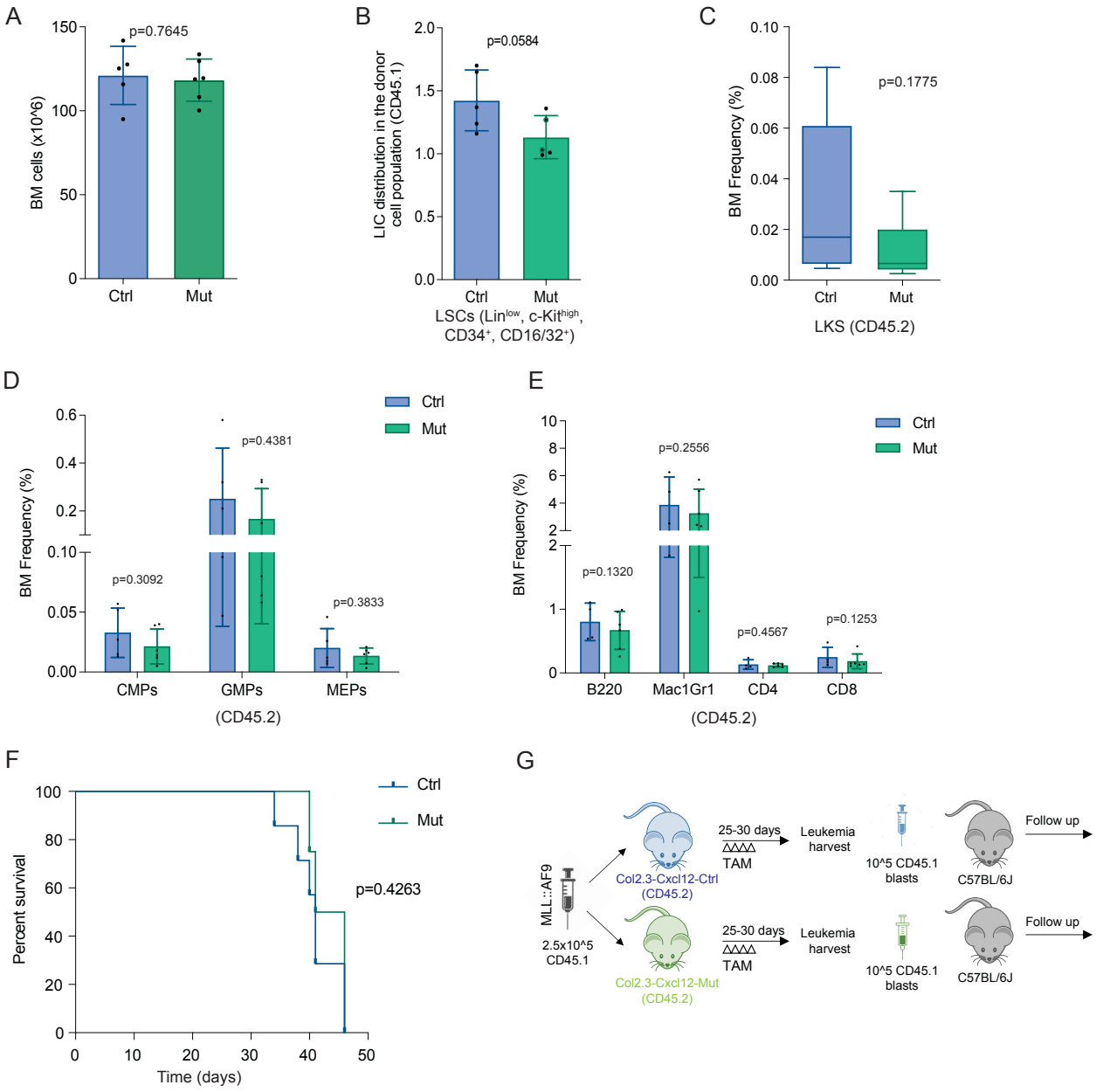

Viñado et al., Supp. Fig. 3

Supplementary Figure 3. CXCL12 produced by mature osteolineage cells is dispensable for AML progression (Related to Fig. 3). (A,B) Bone marrow analysis showing: **(A)** total cellularity and **(B)** Frequency of LSCs (CD45.1$^+$, Lin^{low}, c-Kit^{high}, Sca1$^-$, CD34$^+$, CD16/32$^+$) in the CD45.1 leukemic clone.

(C-E) Bone marrow (BM) analysis showing the frequency of non-leukemic cells (CD45.2): **(C)** Lin^-, $cKit^+$, $Sca1^+$ (LKS) cells; **(D)** common myeloid progenitors (CMPs), granulocyte macrophage progenitors (GMPs) and megakaryocyte erythroid progenitors (MEPs) and **(E)** B220, Mac1-Gr1, CD4 and CD8 cells in the Col2.3-Cxcl12-Ctrl and Col2.3-Cxcl12-Mut mice 30 days after leukemia induction. **(F)** Kaplan-Meier curve showing survival of Col2.3-Cxcl12-Ctrl (n=7) and Col2.3-Cxcl12-Mut (n=4) transplanted with $2x10^5$ MLL::AF9 cells. **(G)** Schematic overview of the experimental design showing serial transplantation of LSCs. TAM denotes the administration of tamoxifen (100 mg/Kg/day, IP) 2 days after leukemia infusion for 4 consecutive days. Data are representative of at least 2 independent experiments. n=5 to 6 mice per genotype per experiment unless otherwise stated. Data are represented as mean and SD. * P< .05; ** P< .01; *** P< .001.

Supp. Figure 4

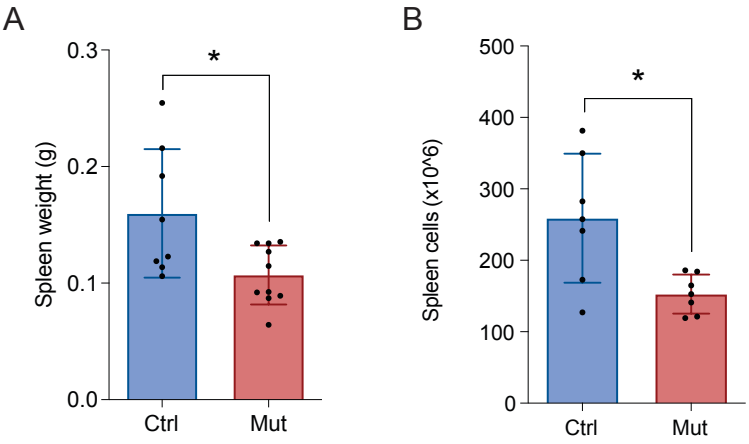

Viñado et al., Supp. Fig. 4

Supplementary Figure 4. Sustained deprivation of CXCL12 produced by Prx1-MSCs does not affect LSC localization in the bone marrow (Related to Fig. 4). (A, B) Spleen analysis showing: **(A)** Spleen weight (g) and **(B)** Spleen cellularity, 25 days post-transplant. Data are representative of at least 2 independent experiments. n=6 mice per genotype per experiment unless otherwise stated. Data are represented as mean and SD. * P< .05; ** P< .01; *** P< .001.

Supp. Figure 5

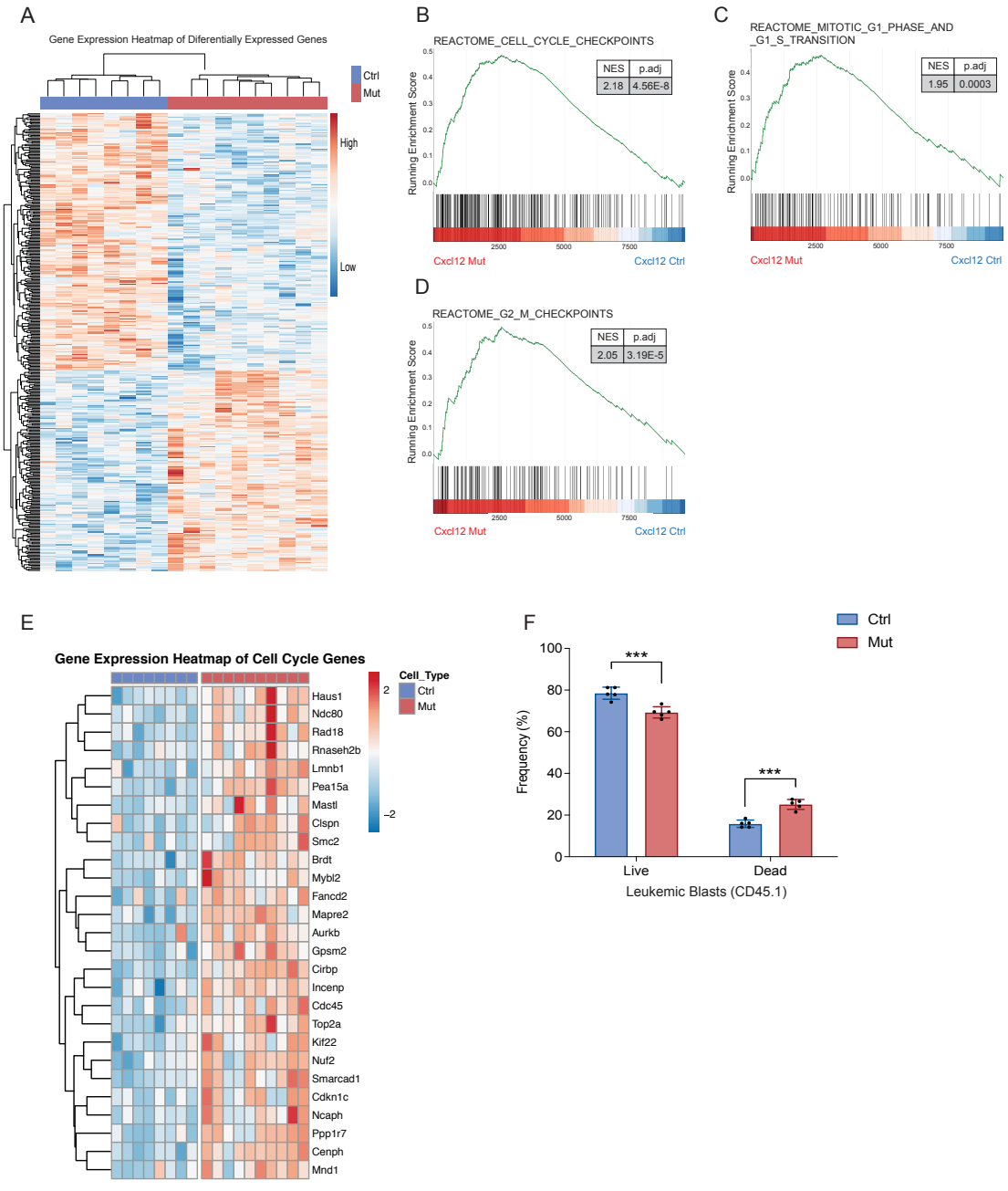

Viñado et al., Supp. Fig. 5

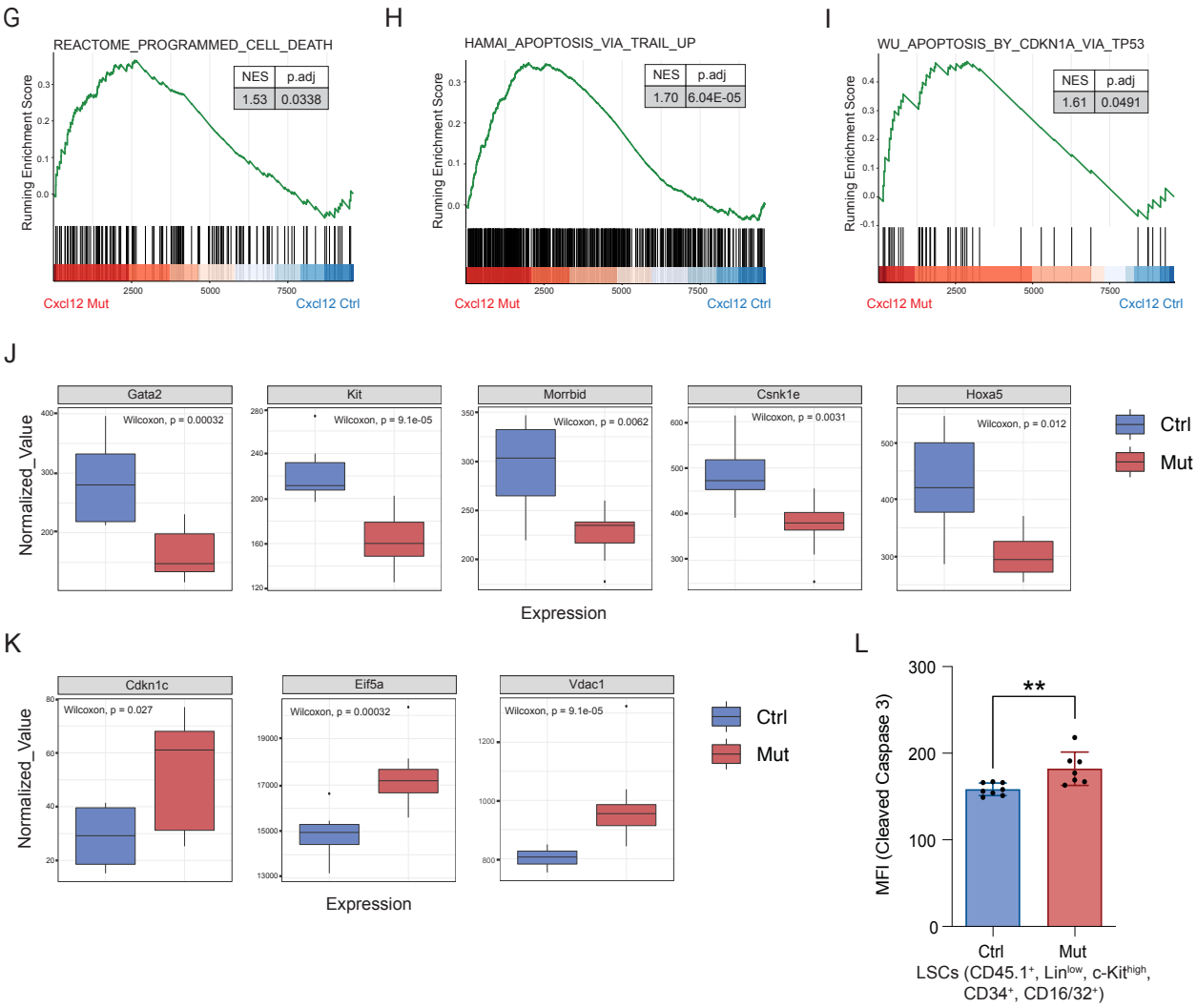

Viñado et al., Supp. Fig. 5 Cont.

Supplementary Figure 5. Mesenchymal stromal cells control cell cycle progression and cell death in LSCs through CXCL12 production (Related to Fig. 5). (A) Heatmap showing the differentially expressed genes from RNA-seq performed on LSCs isolated from the Prx1-Cxcl12-Mut and Prx1-Cxcl12-Ctrl mice. Gene expression is shown in VST-normalized values. **(B-D)** GSEA of the transcriptional signature of LSCs showing an enrichment in signatures related to **(B)** cell cycle checkpoints; **(C)** G1-S transition and **(D)** G2-M transition in LSCs isolated from the Prx1-

Cxcl12-Mut mice. **(E)** Heatmap showing the differentially expressed genes from RNA-seq performed on LSCs isolated from the Prx1-Cxcl12-Mut and Prx1-Cxcl12-Ctrl mice related to mitotic chromosome organization and regulation of cell cycle transition. Gene expression is shown in VST-normalized values. **(F)** Cell death measured by Annexin-V, TO-PRO-3 staining in CD45.1^{+} leukemic cells from the Prx1-Cxcl12-Mut and Prx1-Cxcl12-Ctrl mice. **(G-I)** Gene set enrichment analysis (GSEA) of the transcriptional signature of LSCs showing an enrichment in signatures related to **(G)** programmed cell death; **(H)** apoptosis via Trail and **(I)** p53-dependent apoptosis mediated by p21 in LSCs from the Prx1-Cxcl12-Mut mice (NES: Normalized enrichment score). **(J)** Differential expression of genes associated with survival in LSCs from the Prx1-Cxcl12-Mut and Prx1-Cxcl12-Ctrl mice. **(K)** Differential expression of genes associated with mitochondria mediated apoptosis in LSCs from the Prx1-Cxcl12-Mut and Prx1-Cxcl12-Ctrl mice. **(L)** Apoptosis measured by cleaved caspase 3 staining in LSCs from the Prx1-Cxcl12-Mut and Prx1-Cxcl12-Ctrl mice. Data are representative of at least 2 independent experiments. n=6 mice per genotype per experiment unless otherwise stated. Data are represented as mean and SD. * P< .05; ** P< .01; *** P< .001**.**

Supp. Figure 6

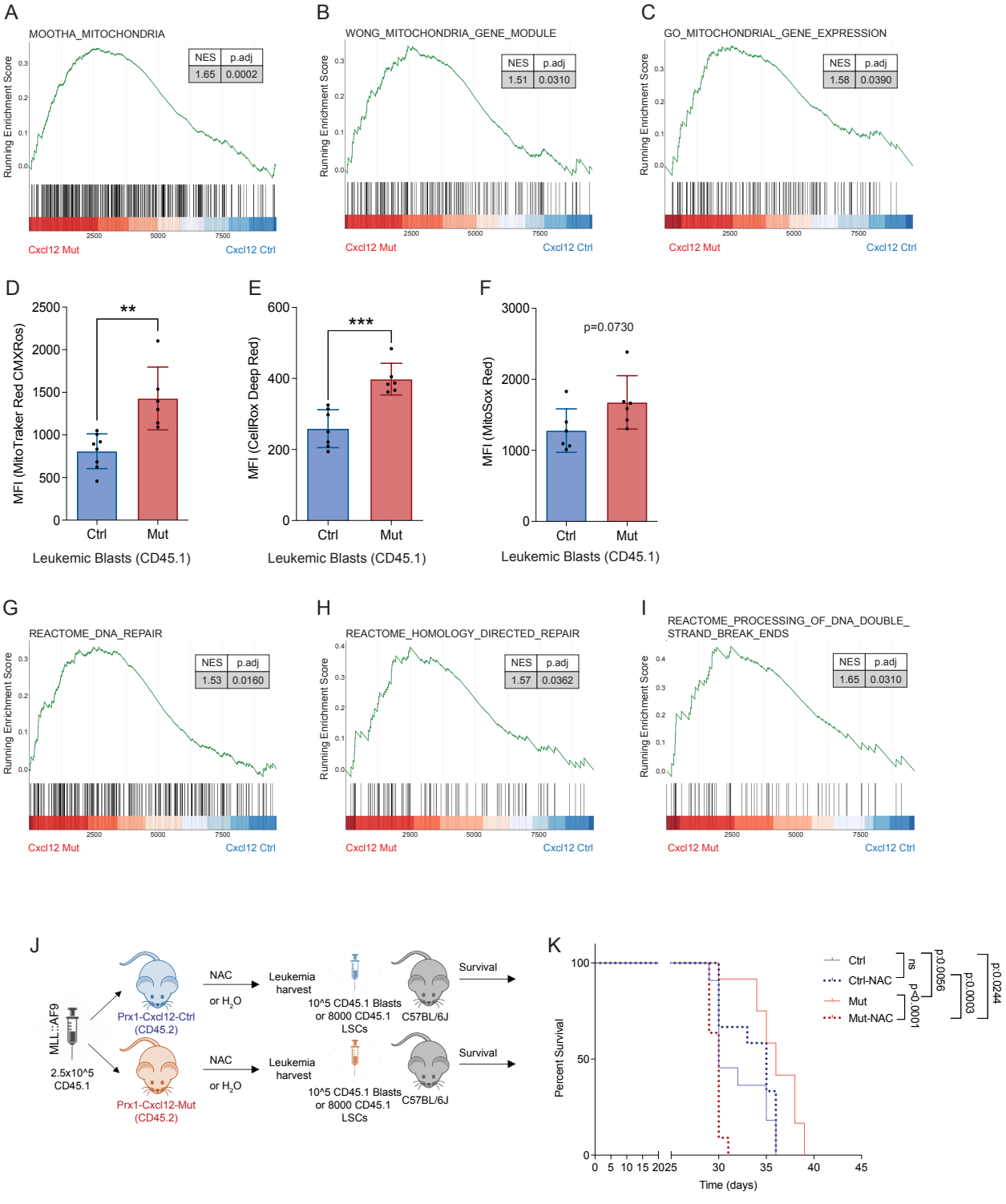

Viñado et al., Supp. Fig. 6

Supplementary Figure 6. Prx1^{+} mesenchymal cells protect LSCs from oxidative stress-induced DNA damage and cell death through CXCL12 production (Related to Fig. 6). (A-C) Gene set enrichment analysis (GSEA) of the transcriptional signature of LSCs suggesting mitochondrial dysregulation in LSCs isolated from the Prx1-Cxcl12-Mut mice. **(D)** Mitochondrial membrane potential of leukemic cells isolated from the Prx1-Cxcl12-Ctrl and Prx1-Cxcl12-Mut mice. **(E,F)** Quantification of **(E)** ROS levels and **(F)** mitochondrial superoxide anion production of leukemic cells isolated from the Prx1-Cxcl12-Ctrl and Prx1-Cxcl12-Mut mice. **(G-I)** GSEA of the transcriptional signature of LSCs showing an enrichment in pathways associated with DNA damage and repair of LSCs isolated from the Prx1-Cxcl12-Mut mice. **(J)** Schematic overview of the experimental design for serial AML induction in C57BL/6J mice with MLL::AF9 cells isolated from the Prx1-Cxcl12-Ctrl and Prx1-Cxcl12-Mut mice and fed with of N-acetyl-cysteine or vehicle. **(K)** Kaplan-Meier curve showing survival of C57BL6J mice (n=12/group) transplanted with equal numbers of leukemic cells from Prx1-Cxcl12-Ctrl (n=23) and Prx1-Cxcl12-Mut (n=23) animals that were fed NAC (1mg/mL) or vehicle in the drinking water throughout leukemia development. Data are representative of at least 2 independent experiments; n=12 mice per genotype per experiment unless otherwise stated. Data are represented as mean and SD. * P< .05; ** P< .01; *** P< .001.

Supp. Figure 7

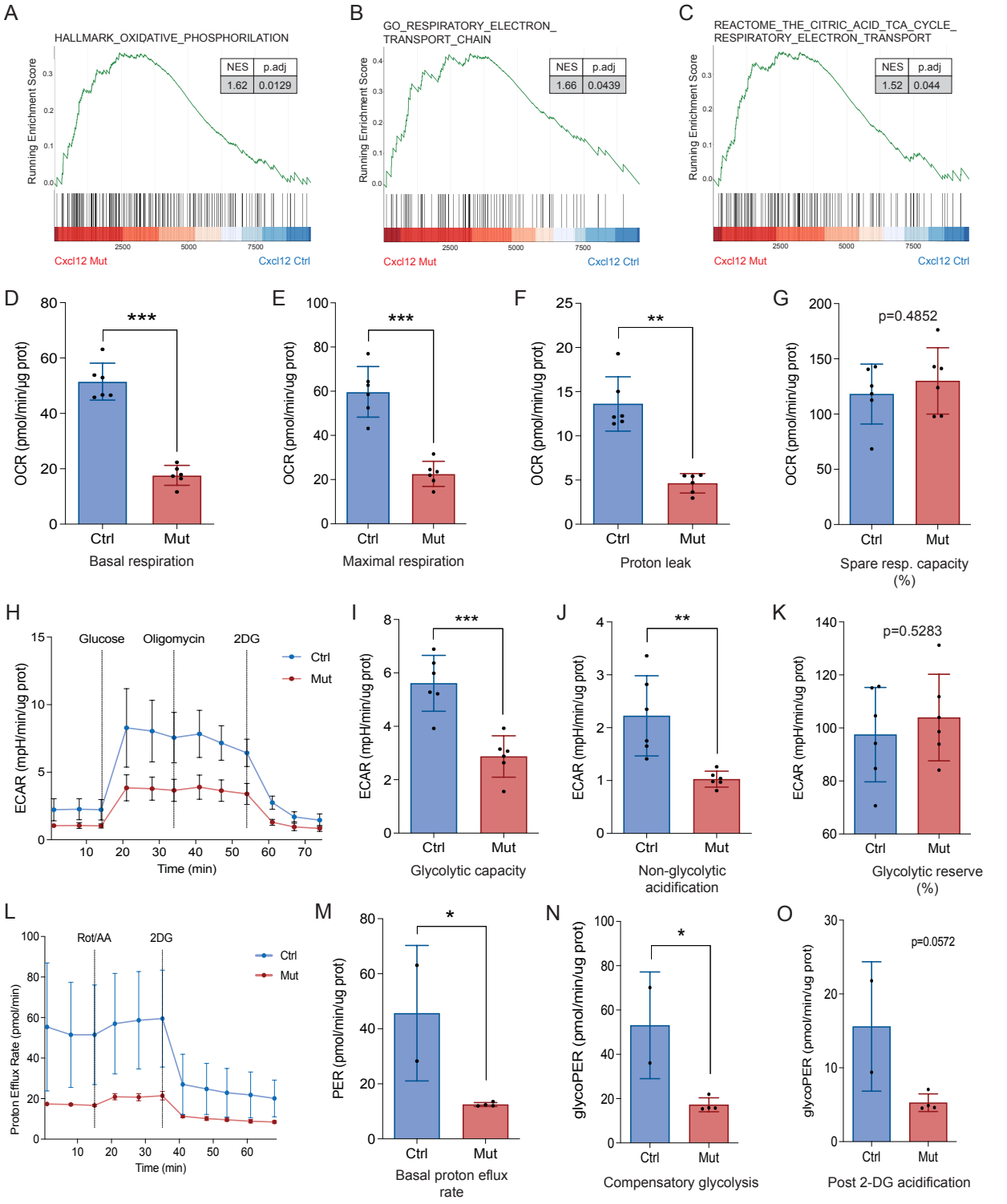

Viñado et al., Supp. Fig. 7

Supplementary Figure 7. Energy metabolism in LSCs is controlled by mesenchymal stromal cells at least in part through CXCL12 production (Related to Fig. 7). (A-C) Gene set enrichment analysis (GSEA) of the transcriptional signature of LSCs showing enrichment in pathways associated with **(A)** oxidative phosphorylation; **(B)** the electron transport chain and **(C)** the TCA cycle in LSCs isolated from the Prx1-Cxcl12-Mut mice. **(D-G)** Seahorse measurement of: **(D)** basal respiration; **(E)** maximal respiration; **(F)** proton leak and **(G)** spare respiratory capacity in LSCs-enriched cells from Prx1-Cxcl12-Mut and Prx1-Cxcl12-Ctrl mice. **(H)** Extracellular acidification rate (ECAR) indicating cellular glycolytic capacity after glucose, oligomycin and 2DG treatment in LSCs-enriched (Lin^-, $CD45.1^+$) cells from Prx1-Cxcl12-Ctrl (n=6) and Prx1-Cxcl12-Mut (n=6) mice. **(I-K)** Seahorse measurement of **(I)** glycolytic capacity; **(J)** non-glycolytic acidification and **(K)** glycolytic reserve, extracellular acidification rate (ECAR) in LSCs-enriched cells from Prx1-Cxcl12-Mut and Prx1-Cxcl12-Ctrl mice. **(L)** Proton efflux from live cells, indicating glycolytic and mitochondrial-derived acidification after Rot/AA and 2DG treatment in LSCs-enriched cells from Prx1-Cxcl12-Ctrl (n=2) and Prx1-Cxcl12-Mut mice (n=4). **(M-O)** Seahorse measurement of **(M)** basal Proton efflux rate (PER), **(N)** compensatory glycolysis and **(O)** post 2-DG acidification in LSCs-enriched cells from Prx1-Cxcl12-Ctrl and Prx1-Cxcl12-Mut mice. Data are representative of at least 2 independent experiments; n= 6 mice per genotype per experiment unless otherwise stated. Data are represented as mean and SD. * P< .05; ** P< .01; *** P< .001.

SUPPLEMENTARY TABLES INFORMATION

Supp. Table 1. Deferentially expressed genes between leukemic cells from pediatric patients showing high (Q4) and low (Q1) transcriptional activity of the CXCR4 pathway (TARGET initiative). Related to Figure 1 and Supp. Figure 1.

Supp. Table 2. Gene set enrichment analysis from RNA-seq performed in leukemic cells from pediatric patients showing high (Q4) and low (Q1) transcriptional activity of the CXCR4 pathway (TARGET initiative). Related to Figure 1 and Supp. Figure 1.

Supp. Table 3. Gene set enrichment analysis from RNA-seq performed in leukemic cells from pediatric patients showing high (Q4) and low (Q1) transcriptional activity of the CXCR4 pathway (Beat AML cohort). Related to Figure 1 and Supp. Figure 1.

Supp. Table 4. Deferentially expressed genes between LSCs from Prx1-Cxcl12-Ctrl and Prx1-Cxcl12-Mut mice. Related to Figure 5 and Supp. Figure 5 and 6.

Supp. Table 5. Gene set enrichment analysis from RNA-seq analysis of LSCs obtained from Prx1-Cxcl12-Ctrl and Prx1-Cxcl12-Mut mice. Related to Figure 5 and Supp. Figures 5-7.

SUPPLEMENTARY EXPERIMENTAL PROCEDURES

Mice

Six to ten weeks old mice from both genders were used for experiments, no animals were excluded from the study. After genotyping mice were randomly assigned to the experimental groups. Sample size was calculated for a a power of 80% and alpha of 0.05 and based on previous knowledge generated in the lab using Gpower and SatsToDo. Personnel performing and analyzing the experiments were blinded to the mouse genotype to reduce potential bias. Deletion of Cxcl12 in Col2.3 mice was achieved by intraperitoneal administration of 100 mg/Kg of tamoxifen (Sigma-Aldrich, Saint Louis, MO, USA) for 4 consecutive days, starting 2 days after AML induction. All animal procedures were performed in accordance with the Institutional and European Union guidelines for Animal Care and Welfare under specific experimental procedures approved by the Institutional Committee on Care and Use of Laboratory Animals of the University of Navarra.

In vivo drug treatment

N-Acetyl-L-Cysteine (NAC)(Sigma-Aldrich, Saint Louis, MO, USA) was administered in the drinking water at a dose of 1 mg/ml, starting 2 days after leukemia infusion for the duration of the experiment.

Complete Blood Count (CBC) analysis

For complete blood count (CBC) analysis, 20 µL of peripheral blood (PB) was collected by tail vein puncture using EDTA anti-coagulated tubes and analyzed by a Hematology analyzer (LaserCell CVM).

Flow cytometry analysis

PB samples were lysed for 15 minutes at room temperature (RT) in 1X BD FACS Lysis Solution 10X (BD Biosciences, Franklin Lakes, NJ, USA), and mature lymphoid and myeloid cells were identified using the following combination of conjugated antibodies in modified PBS (mod PBS: PBS 1x, 2mM EDTA, 2% FBS and 1x Penicillin-Streptomycin) for 20 minutes on ice: CD45.1-PE-Cy7 (eBioscience, 25-0453-82), CD45.2-FITC (eBioscience, 11-0454-82), Mac1-PE (eBioscience, 12-0112-82), Gr1-APC (Biolegend, 108412), B220-BV421 (Biolegend, 103239), CD4-APC-Cy7 (Biolegend, 100413) and CD8-BV510 (Biolegend, 100751).

For immunophenotypic characterization of hematopoietic cell populations in the BM, bones were crushed in a mortar, filtered through a 70-µM filter to obtain single cell suspensions. Red blood cells were lysed in ammonium chloride solution (ACK) lysis buffer (150mM NH_4Cl, 10mM $KHCO_3$ and 0.1mM Na_2EDTA [pH 7.2-7.4]) for 10 minutes at RT. 10µL of each sample was stained with acridine orange and propidium iodide (AO/PI) solution (Nexcelom Bioscience, Lawrence, MA, USA) for total nucleated cell count, size measurement and viability analysis with Cellometer K2 Image Cytometer (Nexcelom Bioscience, Lawrence, MA, USA). Cells were subsequently stained for 20 minutes on ice in the appropriate volume of mod PBS with the following antibody conjugates: CD45.1-PE-Cy7, CD45.2-BV421, biotin anti-mouse lineage panel (Gr-1, Ter119, CD3e and B220)(Biolegend, 133307), Streptavidin-Pacific Orange (Thermo Fisher Scientific, S32365), CD117-APC or APC-eFluor780 (Pharmingen, 553356 and eBioscience, 11-0341-85 respectively), Sca1-PE (eBioscience, 12-5981-83), CD34-FITC (eBiosciences, 11-0341-85) or BV421 (BD, 562608) and CD16/32-PerCP-Cy5.5 (eBiosciences, 45-0161-82). Dead cells were excluded by staining with 2µL of To-pro-3 Iodide (642/661) (ThermoFisher Scientific, Waltham, MA, USA) or 2µL of Sytox Blue (ThermoFisher Scientific, Waltham, MA, USA). Cell cycle status was evaluated permeabilizing

samples with BD's Cytofix/Cytoperm™ Solution Kit following manufacturer`s recommendations and incubated with Ki-67-FITC (BD Biosciences, Franklin Lakes, NJ, USA) in the dark for 45 minutes on ice, followed by To-pro-3 Iodide (642/661) staining for 10 minutes. Mitochondrial membrane potential (MMP, ΔΨm) was detected by staining cells with Mitotracker Red CMXRos (ThermoFisher Scientific, Waltham, MA, USA) at a final concentration of 50 nM. Reactive oxygen species (ROS) were detected by staining BM cells with CellROX® Deep Red reagent (ThermoFisher Scientific, Waltham, MA, USA) and MitoSOX™ red mitochondrial superoxide indicator (ThermoFisher Scientific, Waltham, MA, USA) following the manufacturer`s recommendations. Cell death assay was performed incubating samples with Annexin V-FITC (BD Pharmingen) and To-pro-3 Iodide (642/661) at a final concentration of 1/20 and 1/40 respectively in 1X Annexin V Binding Buffer 10X (BD Biosciences, Franklin Lakes, NJ, USA) in the dark for 25 minutes at RT. For Caspase 3 activation assay in LSCs, samples were permeabilized with the BD Solution Kit following manufacturer`s recommendations and incubated with PE labeled anti-active caspase 3 (BD Biosciences, Franklin Lakes, NJ, USA) at 1/6 in 1X BD Perm/Wash™ buffer for 30 minutes in the dark at RT. All data collection was performed on a FACS-CANTO or FACS Aria II (Beckon Dickinson, Franklin Lakes, NJ, USA) and data analysis was performed with FlowJo (BD Biosciences, Franklin Lakes, NJ, USA).

Immunofluorescence detection of γH2AX

CD45.1 leukemic cells and LSCs were FACS sorted and fixed with 4% paraformaldehyde (PFA, Sigma-Aldrich, Saint Louis, MO, USA). Cytospin preparations were blocked and permeabilized using PBS-1% BSA and 0.1% Triton X-100 (Sigma-Aldrich, Saint Louis, MO, USA) respectively. Samples were incubated with primary Phospho-Histone H2A.X (Ser139) (20E3) rabbit antibody

(Cell Signaling, Danvers, MA, USA) diluted 1/200 in blocking solution overnight at 4ºC. After washing, Alexa Fluor 594 anti-rabbit IgG secondary antibody (ThermoFisher Scientific, Waltham, MA, USA) diluted 1/300 in blocking solution was incubated for 60 minutes at RT. Nuclei were counterstained with DAPI 1:1000 (ThermoFisher Scientific, Waltham, MA, USA). Samples were imaged using a Zeiss LSM 510 META laser confocal microscope (Carl Zeiss, Jena, Germany) and analyzed using ImageJ/Fiji (NIH).

Seahorse metabolic extracellular flux profiling

The oxygen consumption rate (OCR) was measured under basal conditions, and in response to Oligomycin (1 µM), Trifluorocarbonylcyanide Phenylhydrazone (FCCP; 1.5 µM) and the combination of Rotenone and Antimycin A (Rot/AA 0.5 µM). The extracellular acidification rate (ECAR) was detected after injection of Glucose (5 mM), Olygomicin (1 µM) and 2-Deoxyglucose (2-DG, 50 mM). The Proton efflux rate (PER) was measured after Rot/AA (0.5 µM) and 2-DG (50 mM) injections. Data presented were normalized to total protein amount per well. Wafe software (version 2.6.1.53) was used for data analysis.

RNA Isolation and qPCR

RNA isolation was performed using TRI Reagent (Sigma-Aldrich). Reverse transcription was performed using PrimeScript RT reagent Kit (Takara, Kusatsu, Japan), following the manufacturer's recommendations. qPCR was performed using the PowerUp SYBR Green Master Mix (Applied Biosystems, Waltham, MA, USA) and QuantStudio 5 Real Time PCR System (Thermo Fisher Scientific, Waltham, MA, USA). The sequences of the primers used were as follows: mouse *Cxcl12* forward: TGCATCAGTGACGGTAAACCA; reverse: CACAGTTTGGAGTGTTGAGGAT.

Profiling by RNA-Seq

Seven thousand LSCs from 10 mice and 2 technical replicates from each one, were sorted in Lysis/Binding Buffer (Thermo Fisher Scientific, Waltham, MA, USA). Poly-A RNA was selected with Dynabeads Oligo (dT) (Thermo Fisher Scientific, Waltham, MA, USA) and reverse-transcribed with AffinityScript Multiple Temperature Reverse Transcriptase (Agilent Technologies, Santa Clara, CA, USA) using poly-dT oligos carrying a 7 bp-index. Up to 8 samples with similar overall RNA content were pooled together and subjected to linear amplification by IVT using HiScribe T7 High Yield RNA Synthesis Kit (New England Biolabs, Ipswich, MA, USA). Next, RNA was fragmented into 250-350 bp fragments with RNA Fragmentation Reagents (Thermo Fisher Scientific, Waltham, MA, USA) and dephosphorylated with FastAP (Thermo Fisher Scientific, Waltham, MA, USA) following manufacturer´s instructions. Partial Illumina adaptor sequences were ligated with T4 RNA Ligase 1 (New England Biolabs, Ipswich, MA, USA), followed by a second RT reaction. Full Illumina adaptor sequences were added during final library amplification with KAPA HiFi DNA Polymerase (Kapa Biosystems, Potters Bar, UK). RNA-Seq libraries quality controls consisted in quantification with Qubit 3.0 Fluorometer (Life Technologies, Carlsbad, CA, USA) and size profile examination with Agilent's 4200 TapeStation System. Libraries were sequenced in an Illumina NextSeq 500 at a sequence depth of 10 million reads per sample.

Bioinformatic Analysis

Mice gene expression profiles were obtained from FASTQ files using Salmon 1.3.0. Human gene expression datasets were obtained from TARGET-AML(1) and BEAT-AML(2) databases. R 3.5.3 and 4.0.1 were used for the remaining downstream analysis. For the transcriptional analysis of

mouse LSC DESeq2(3) recommended workflow was used to perform normalization and differential gene expression analysis. Genes with a FDR adjusted p-value < 0.05 were considered as differentially expressed. Gene Ontology (GO) enrichment analysis was performed via ClusterProfiler package together with a Gene Set Enrichment Analysis (GSEA) based on the Molecular Signatures Database collections(4-6).

For human datasets, Graphite(7) package was used to identify the genes involved in the CXCR4 pathway. The normalized expression of the resulting genes was summed up and computed a ranking was computed with all the samples. Samples were kept in the first (lower expression) and fourth (higher expression) quartiles for further analysis, as a proxy for the CXCL12 ligand stimulation. Differential gene expression analysis, GO and GSEA analyses were performed between the aforementioned groups as explained above.

The R versions 3.5.3 and 4.0.1 were used for the analysis, as well as the following R packages: survminer_0.4.9, survival_3.2-10, org.Hs.eg.db_3.12.0, reactome.db_1.74.0, graphite_1.36.0, ggrepel_0.9.1, ggfortify_0.4.11, ggpubr_0.4.0, pheatmap_1.0.12, dplyr_1.0.5, org.Mm.eg.db_3.12.0, AnnotationDbi_1.52.0, factoextra_1.0.7, ggplot2_3.3.3, DESeq2_1.30.1, SummarizedExperiment_1.20.0, Biobase_2.50.0, MatrixGenerics_1.2.1, matrixStats_0.58.0 gskb_1.22.0, msigdbr_7.2.11, fgsea_1.16.0, biomaRt_2.46.3, rtracklayer_1.49.5, GenomicRanges_1.42.0, GenomeInfoDb_1.26.7, IRanges_2.24.1, S4Vectors_0.28.1, BiocGenerics_0.36.0, tximport_1.18.0.

The results published here are in whole or part based upon data generated by the Therapeutically Applicable Research to Generate Effective Treatments (https://ocg.cancer.gov/programs/target)

initiative, phs000465. The data used for this analysis are available at https://portal.gdc.cancer.gov/projects. Code used in this study will be made available to the community upon request.

Statistical analysis

Statistical analyses were performed using GraphPad Prism 8 and R -software. Data represent the mean and standard deviation or median and IQR of at least two independent experiments. P values below 0.05 were considered statistically significant. Normality was assessed using Shapiro-Wilk test. Levene´s test was used to assess homoscedasticity. For parametric group comparisons, Student t-test or ANOVA (with the appropriate posthoc test) were used. For non-parametric group comparisons Mann-Whitney U test or Kruskal-Wallis were used.

SUPPLEMENTARY REFERENCES

1. Farrar JE, Schuback HL, Ries RE, Wai D, Hampton OA, Trevino LR, et al. Genomic Profiling of Pediatric Acute Myeloid Leukemia Reveals a Changing Mutational Landscape from Disease Diagnosis to Relapse. Cancer Res. 2016;76(8):2197-205.
2. Tyner JW, Tognon CE, Bottomly D, Wilmot B, Kurtz SE, Savage SL, et al. Functional genomic landscape of acute myeloid leukaemia. Nature. 2018;562(7728):526-31.
3. Love MI, Huber W, Anders S. Moderated estimation of fold change and dispersion for RNA-seq data with DESeq2. Genome Biol. 2014;15(12):550.
4. Liberzon A, Subramanian A, Pinchback R, Thorvaldsdottir H, Tamayo P, Mesirov JP. Molecular signatures database (MSigDB) 3.0. Bioinformatics. 2011;27(12):1739-40.
5. Liberzon A, Birger C, Thorvaldsdottir H, Ghandi M, Mesirov JP, Tamayo P. The Molecular Signatures Database (MSigDB) hallmark gene set collection. Cell Syst. 2015;1(6):417-25.
6. Subramanian A, Tamayo P, Mootha VK, Mukherjee S, Ebert BL, Gillette MA, et al. Gene set enrichment analysis: a knowledge-based approach for interpreting genome-wide expression profiles. Proc Natl Acad Sci U S A. 2005;102(43):15545-50.
7. Sales G, Calura E, Cavalieri D, Romualdi C. graphite - a Bioconductor package to convert pathway topology to gene network. BMC Bioinformatics. 2012;13:20.